Determination of appropriate land use/cover pattern based on the mitigating drying effects to support ecohydrological sustainability in the agro-pastoral ecotone of northwest China

Yuzuo Zhu[1], Xuefeng Xu[1]

[1] Key Laboratory of West China's Environmental System (Ministry of Education), College of Earth and Environmental Sciences, Lanzhou University, Lanzhou, Gansu 730000, China

Correspondence to: Yuzuo Zhu (zhuyz16@lzu.edu.cn)

Abstract. The Chinese government has implemented large-scale vegetation restoration projects and plans to expand the percentage of grasslands to 60 %. However, excessive vegetation restoration consumes more moisture and causes soil drying in the agro-pastoral ecotone of Northwest China (APENWC). The optimal mixture of land use/cover in the APENWC incorporated into vegetation restoration strategies to mitigate the drying effects remains unclear. To fill this gap, the Community Land Model version 5.0 (CLM5.0) with static climatic forcing was used to analyse the spatially averaged impacts of land use/cover change (LUCC) by simulating real LUCC scenarios from 2000 to 2015 and examine the impacts of different types of LUCC by simulating idealised maximised LUCC scenarios. The results showed that the two main types of LUCC in the study region from 2000 to 2015 were the conversion from bare land and croplands to grasslands. The bare land to grasslands decreased the annual mean land surface temperature (LST) by -0.17 °C, while croplands to grasslands increased the yearly mean LST by 0.96 °C; evapotranspiration (ET) changes were 53.32 and -184.42 mm yr^{-1}, respectively, leading to an annual spatially averaged LST by a cooling range of -0.06 ± 0.15 °C and ET increased by a range of 9.70 ± 19.04 mm yr^{-1} in the study region. The correlation coefficients between biogeophysical characteristics and change of ET and LST indicated that surface albedo was the most sensitive surface characteristic influencing LST and ET in summer and winter from bare land and croplands to grasslands. In contrast, the leaf and stem area index (LAI + SAI) showed the most significant correlation between croplands and grasslands throughout the year. An analysis of changes in land use/cover patterns from 2000 to 2015 found that some grids experienced drying and warming as vegetation restoration projects, owing to the offsetting effects of the two types of LUCC. Furthermore, to identify the proper land use/cover pattern to mitigate drying, we designed different LUCC scenarios by varying the mixture of land use/cover in the CLM5.0 and compared the criteria (water conservation and LST) from the output. Based on higher water conservation and cooling surface, results show that the optimal percentages of grasslands, bare land, and croplands in the APENWC approximately are 60, 23, and 11 %, respectively, which will mitigate the drying and warming surface environment; this suggests that approximately 5348 km^2 of bare land and 1163 km^2 of croplands will be transformed into grasslands. These findings provide vital information for maintaining ecohydrological sustainability in the APENWC and similar areas.

Keywords: Land use/cover change, Water conservation, CLM5.0, Land use pattern, Agricultural-pastoral ecotone in Northwest

1 Introduction

Land use/cover change (LUCC), such as deforestation, afforestation, grassland restoration, and agricultural expansion, affects the interaction of energy and vapour at the interface between the land and atmosphere by modifying biogeophysical characteristics, thereby modulating climate and hydrology at regional and global scales (Alkama and Cescatti, 2016; Chen and Dirmeyer, 2016; Chen and Dirmeyer, 2017; Davin et al., 2020; Duveiller et al., 2018; Liu et al., 2016; Woodward et al., 2014). The LUCC has been recognised as one of the key climatic, hydrological mitigation, and adaptation strategies available to governments, especially under global warming and water resource shortages (Arora and Montenegro, 2011; Davin et al., 2014; Findell et al., 2017; Poniatowski et al., 2020). Therefore, examining the impacts of the LUCC and developing optimal land use/cover patterns are crucial for supporting long-term sustainable land management and ecosystem services (Jia et al., 2017a; Zhang et al., 2018).

Statistical analyses based on in-situ observations, satellite products, and simulated scenarios using numerical models have been widely adopted (Lee et al., 2011; Nkhoma et al., 2021). However, in-situ observations are sparsely and unevenly distributed because of equipment and resource constraints (Li et al., 2021; Zhang et al., 2021). Satellite products rarely provide accurate continuous long-term data because the satellites obtains instantaneous images, and processing methods introduce uncertainty (Srivastava et al., 2015; Zhang et al., 2010). Numerical models have been used to study multiple variables with high spatial resolution over extended periods and to access flux cycles with a consistent framework (Han et al., 2021; Winckler et al., 2018). Many studies have used numerical models to systematically interpret water and energy processes, contributing to a better understanding of the impacts of LUCC (Chen and Dirmeyer, 2019; Llopart et al., 2018). The Community Land Model (CLM), in which each grid cell is composed of multiple land use/cover, represents well under different land use/cover and LUCC regions (Li, 2021; Meier et al., 2018; Xu et al., 2020; Lawrence et al., 2019), which would effectively simulate changes in the water and energy processes response to LUCC.

Land surface temperature (LST) and evapotranspiration (ET) are extremely sensitive to the LUCC and provide important information regarding extreme events and water resource management (Chen and Dirmeyer, 2018; He et al., 2020; Li et al., 2015; Wang et al., 2020). The impacts of the LUCC on LST vary mainly because of competition among different biogeophysical characteristics, such as surface albedo and surface roughness (Burakowski et al., 2018; Cherubini et al., 2018; Davin and De Noblet-Ducoudré, 2010; Li et al., 2015). The LUCC alters the redistribution of moisture flux and energy balance through biogeophysical characteristics, which differ according to LUCC types and spatial variability, leading to impacts on ET (Das et al., 2018; Li et al., 2017; Ning et al., 2017; Winckler et al., 2017). Additionally, the diurnal cycle has been widely adopted to clearly show discrepancies in flux distribution, including soil residual heat fluxes and latent heat fluxes, representing temperature and ET, in different land use/cover types, and to explicitly explain how biogeophysical

characteristics in the LUCC process affect the energy and water cycle (Breil et al., 2020; Kueppers and Snyder, 2011). However, the spatially averaged impacts of LUCC and the impacts of a single LUCC on LST and ET have been studied extensively (Cherubini et al., 2018; Davin and De Noblet-Ducoudré, 2010), and few researchers have quantified and attributed these spatially averaged impacts to the synergy of different LUCC types under complicated realistic conditions. Therefore, LST and ET were selected as representatives to quantify the synergy and respective impacts of different types of LUCC, which will help explain the mechanisms of optimal land use/cover patterns.

The agricultural pastoral ecotone in Northwest China (APENWC), which is mainly interlaced by grasslands, croplands, and bare land, is one of the largest agropastoral ecotones worldwide (Li et al., 2018; Xue et al., 2019; Yang et al., 2021a). Since the 1980s, The land surface vegetation has been experiencing changes over the last decades due to implemented policies, such as the "Grain for Green Project" and "Three-North Shelterbelt" (Cao et al., 2015; Wei et al., 2018; Liu et al., 2019). These programs have contributed to increased vegetation (Wang et al., 2019b; Wu et al., 2013; Xue et al., 2019; Zhang et al., 2018) and vegetation restoration has led to increased soil moisture consumption (Yang et al., 2021a), reduced runoff (Liang et al., 2015; Zhang et al., 2016), increased ET (Wang et al., 2019a) and decreased LST (Wang et al., 2020). However, some studies have pointed out that excessive vegetation restoration declines ecohydrological sustainability, such as soil drying (Jia et al., 2017b; Zhang et al., 2018), indicating that incorporating proper land use/cover into decision-making suitable for the APENWC standing perspective of ecohydrological sustainability is urgently required. Additionally, the latest national ecological development project plans to expand the percentage of grasslands to 60 % in China and continue to convert bare and agricultural lands to grasslands to improve ecosystem services in the APENWC from 2021 to 2035 (China state council, 2017; National development and reform commission, 2019). However, this plan to expand the percentage of grasslands to 60 % of the study area has not been robustly tested, and little was done to propose the proper percentages of croplands and bare land suitable for the APENWC under the government plan.

This study identifies the optimal mixture of land use/cover to expand the percentage of grasslands to 60 % and mitigate the drying effects due to vegetation restoration, for the first time. Previous studies have optimised land use/cover by setting different weights for economic profit and ecological parameters in scenario simulations using a Multi-Objective Genetic Algorithm(Kaim et al., 2018; Kucsicsa et al., 2019; Yang et al., 2020). The experimental design was limited owing to insufficient theoretical studies on parameter settings (Ding et al., 2021) and could not meet the government's preset values (e.g., 60 % grassland). Therefore, we first quantified the impacts of the LUCC by simulating land uses/cover scenarios with static climatic forcing in the CLM. We investigated the spatially averaged impacts of LUCC in real scenarios from 2000 to 2015, as well as the impacts of a single type of LUCC in idealised scenarios with maximised LUCC. These spatially averaged impacts were attributed to the synergy of different LUCC types. In addition, we further designed different LUCC scenarios by setting the percentage of grasslands as 60 % and varying the percentages of croplands and bare land in the CLM5.0 to identify the optimal mixture of land use/cover in the APENWC based on the higher water conservation and cooling surface.

2 Materials and Methods

2.1 Study area

The boundary of the agro-pastoral ecotone did not reach agreement because of the differently defined indicators of ecology, climatology, and economic geography (Li et al., 2021). The APENWC was identified based on previous research(Wang et al., 2020; Tan et al., 2020), including the Otog Banner, Otog Front Banner, Lingwu, Yanchi, Dingbian, Jingbian, Hengshan, Yuyang, Wushen, and Shenmu. It is located northwest of the agro-pastoral ecotone in Northern China (APENC). It lies between 36.816 to 40.194 °N and 106.228 to 110.903 °E (Fig. 1), covering 77,513 km², at an elevation of 915–1947 m above mean sea level with an annual average temperature of 7.0 to 9.0 °C, an annual average relative humidity of 13 %, and annual precipitation of 250 to 450 mm with most of it falling in the summer (Xu et al., 2020; Yang et al., 2021a). The sequence's dominant land use/cover types were grasslands, bare land, and croplands. The study area is a climatic and ecological transition belt historically developed by agricultural cultivation and animal husbandry. It is highly sensitive to changes in human activities and background climate (Tan et al., 2020; Wei et al., 2018; Xue et al., 2019).
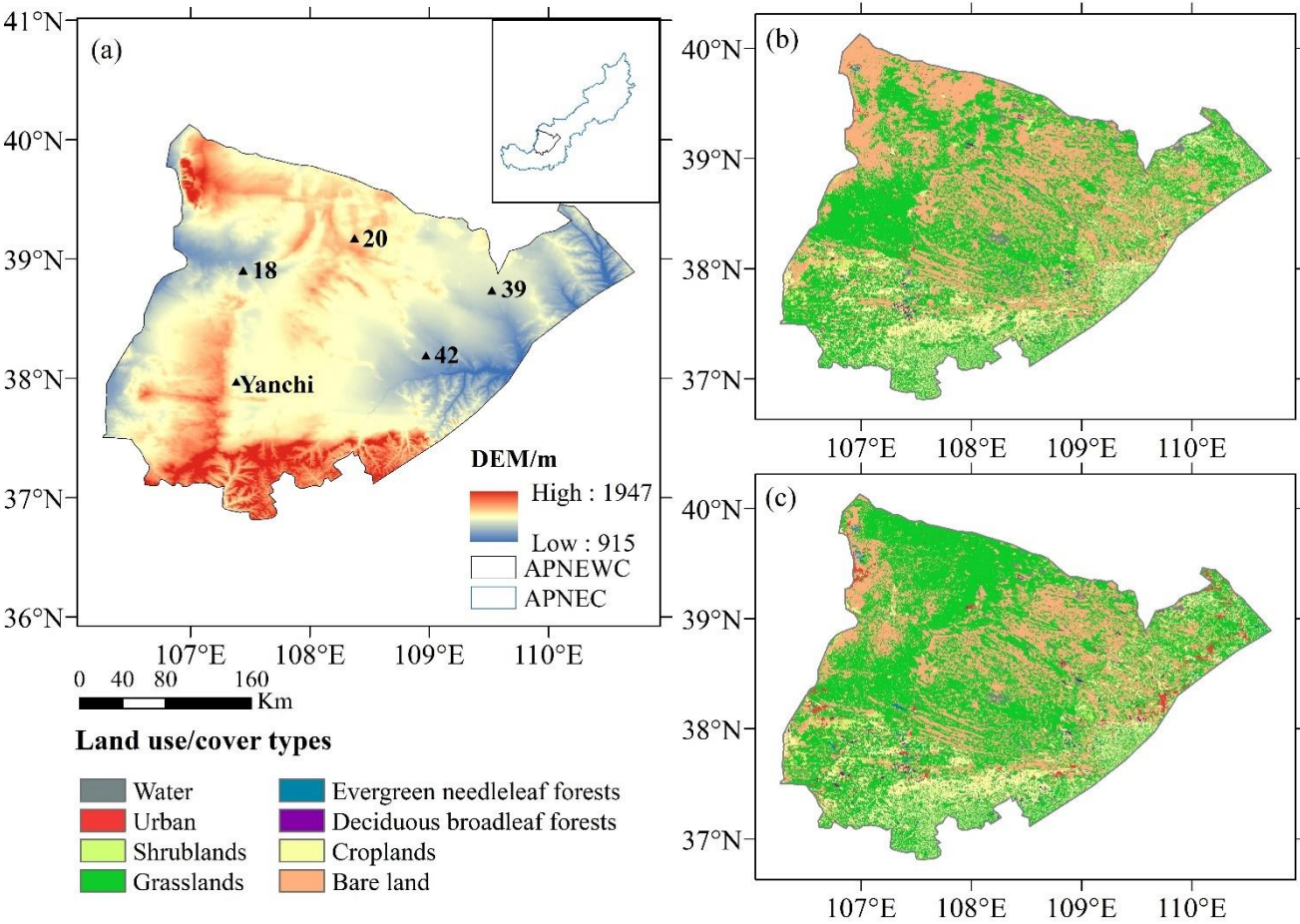
Figure 1. (a) DEM of the APNEWC and the locations of the in-situ observation stations. (b) Land use/cover map of the study area in 2000. (c) Land use/cover map of the study area in 2015.

2.2 Datasets

The surface land use/cover dataset covered the study area with a 30 m ×30 m resolution. Two years 2000 and 2015 were selected to represent land use/cover before and after the vegetation restoration projects. The land use/cover dataset over the APENWC contains eight land use/cover types, including shrublands, grasslands, croplands, urban areas, barren land, water bodies, evergreen needleleaf forests, and deciduous broadleaf forests, which correspond to the land use/cover types in the CLM5.0 input surface data. Rainfed and irrigated croplands data were calculated using the ratio of irrigated land to cultivated land in the Shanxi, Ningxia, and Erdos Yearbooks. The percentage of rainfed and irrigated croplands on the APENWC was 61.30 and 38.70 in 2000, and 46.48 and 53.52 in 2015, respectively (Xu, 2018; Yang, 2021). The China meteorological forcing dataset (CMFD, http://data.tpdc.ac.cn), with a 3-hour time step and a horizontal spatial resolution of 0.1 °, covers the period from 1979 to 2018 (Yang and He, 2016), widely. The soil properties dataset for land surface modelling over China (http://data.tpdc.ac.cn) with a 30×30 arcsec resolution included sand, clay, soil organic matter, and bulk density (Shangguan and Dai, 2013).

Six in-situ observation stations were established in 2016. Two Yanchi sites were used for croplands and grasslands, site 18, site 20, site 39 for grasslands, and site 42 for croplands. The sampling locations are shown in Fig. 1 and Table S1. The latitude, longitude, and elevation were determined using a GPS receiver during the field survey. Soil temperature and moisture were recorded every half hour from August 2016 using an ECH20 sensor to record the 0–5, 5–10, 10–15, 15–30, and 30–50 cm soil layers. The MODIS LST (https://lpdaac.usgs.gov/dataset_discovery/modis) with 0.05 ° spatial resolution was used to validate LST over the domain, including daytime and nighttime (Wan et al., 2015). ET and net radiation were validated over the domain using two sensing products from GLASS (http://glass-product.bnu.edu.cn/): ET with 8-day temporal resolution and 0.05 ° spatial resolution and surface all-wave daily net radiation with daily temporal resolution and 0.05 ° spatial resolution (Guo et al., 2020; Yao et al., 2014).

Table S2 lists the input and validation datasets, product names, and support resources. The surface land use/cover dataset that covered the study area was evaluated in a previous study and its precision was reliable (Du et al., 2020). The China meteorological forcing dataset and MODIS LST have been widely used in the study area of previous studies (Li, 2021; Wang et al., 2020). Other datasets, such as GLASS have been evaluated in papers that produce the data. The uncertainty in soil properties is discussed in Section 4.2. For the convenience of model validation, we interpolated all data into 0.1 ° grids coincident with the spatial resolution of the model output.

2.3 Model description and experimental design

CLM5.0, developed by the National Center for Atmospheric Research (NCAR) and serving as the land surface component of the Community Earth System Model (CESM, http://www.cesm.ucar.edu/models/cesm2/), is a land surface model including

biogeophysical and biogeochemical processes (Lawrence et al., 2019). In CLM5.0, each grid cell has different land units, including vegetated, crop, lake, urban areas, and glacier. The vegetated land unit is divided into 16 plant functional types (PFTs) in the SP compset (Bonan et al., 2002; Lawrence et al., 2019). Details of the latest CLM5.0 adopted in this study can be found in the technical description in version 5.0 (http://www.cesm.ucar.edu/models/cesm2/land/CLM50_Tech_Note.pdf).

145 Because we needed to represent the local crop of APNEC in CLM5.0, we modified the parameters of the C3 Unmanaged Crop in the SP compset and regarded it as corn. According to the local corn in the APNEC, the modifications in this study include: leaf area index (LAI) of 0 as a managed crop in the non-growing season, canopy height of corn of 1.65 m by field gauge from 2017 to 2018, C4 photosynthetic pathway because corn is a C4 plant, and stem area index (SAI) of 0.1* LAI.

The entire domain was produced in CLM5.0 with 40×50 horizontal grid cells with a spacing of 0.1 ° and each grid was

150 composed of percentages of multiple land use/cover. The spin-up time to reach equilibrium was strictly constrained by $|Var_{n+1}-Var_n| < 0.001*|Var_n|$ (Cai et al., 2014; Yang et al., 1995), where Var is each of the variables for the spin-up and n is the year for the spin-up time. According to Han et al. (2021), soil moisture requires the longest memory time. Therefore, the soil moisture was selected as the constrained variable (Fig. S1). We cycled atmospheric forcing from 1979 to 2018 twice to run the spin-up. Thus, the results for 2000 and 2015 reached an equilibrium and were used in the analysis.

155 A suite of numerical simulations is described in Table 1 to evaluate CLM5.0 and to explore the impacts of LUCC. First, single-point simulations with maximised single land cover/use were compared with in-situ observations to assess the performance of CLM5.0 under different land use/cover conditions. CN2000 and CN2015 simulated the actual land surface and atmospheric forcing and were then used to assess the accuracy of CLM5.0 over the entire domain. The impacts of the LUCC were examined using the differences between EXP2000 and CN2015, isolating the impacts caused by the LUCC

160 from 2000 to 2015 (Wang et al., 2020). In the EXP_bare and EXP_crop scenarios, the bare land and croplands were extended by 100 %, respectively. Subsequently, in the EXP_grass scenario, grasslands were set to 100 % to replace bare land and croplands (Cherubini et al., 2018). Thus, EXP_grass, EXP_bare, and EXP_crop were simulated with maximised land use/cover further to analyse the impacts of the different types of LUCC. To explore a proper mixture of land use/cover in the APENC, we set the percentage of grasslands as 60 % and varied the percentages of croplands and bare land in EXP_602113,

165 EXP_602311, EXP_602509, EXP_602707, and EXP_603004. In addition, two sensitivity experiments were conducted to examine the role of the biogeophysical characteristics of vegetation. The leaf and stem area index (LAI + SAI) of grasslands was replaced by crops in Yanchi_laisai and canopy height in Yanchi_height (Breil et al., 2020). Sensitivity experiments were conducted only at the most representative Yanchi station to reduce computation time.

Table 1. List of numerical simulations.

Experiment	Region/points	Land use/land cover	Atmospheric Forcing	Grid
Yanchi_grass	Yanchi	grasslands	2015-2018	0.0001 °
Yanchi_crop	Yanchi	croplands	2015-2018	0.0001 °
18_grass	18	grasslands	2015-2018	0.0001 °
20_grass	20	grasslands	2015-2018	0.0001 °
39_grass	39	grasslands	2015-2018	0.0001 °
42_crop	42	croplands	2015-2018	0.0001 °

CN2000	Domain	2000	2000	0.1 °	170
CN2015	Domain	2015	2015	0.1 °	
EXP2000	Domain	2000	2015	0.1 °	
EXP2015	Domain	2015	2000	0.1 °	
EXP_grass	Domain	Grasslands	2015	0.1 °	
EXP_bare	Domain	Bare land	2015	0.1 °	
EXP_crop	Domain	Croplands	2015	0.1 °	
EXP_602113	Domain	grasslands60%, bare land 21%, croplands13%	2000-2015	0.1 °	
EXP_602311	Domain	grasslands60%, bare land 23%, croplands11%	2000-2015	0.1 °	175
EXP_602509	Domain	grasslands60%, bare land 25%, croplands9%	2000-2015	0.1 °	
EXP_602707	Domain	grasslands60%, bare land 27%, croplands7%	2000-2015	0.1 °	
EXP_603004	Domain	grasslands60%, bare land 30%, croplands4%	2000-2015	0.1 °	
Yanchi_laisai	Yanchi	Yanchi	2015	0.0001 °	
Yanchi_height	Yanchi	Yanchi	2015	0.0001 °	

2.4 Model evaluation

Previous work have validated the soil moisture output of CLM5.0 under grasslands and croplands in the APENWC compared to in-situ observations (Li, 2021). The simulated soil temperature in grasslands and croplands agreed with the in-situ observations (Fig. S2). The correlation coefficient (R) values for Yanchi grass, Yanchi crop, 18, 20, 39, and 42 were 0.98, 0.98, 0.99, 0.96, 0.97, and 0.96, respectively. The BIAS (absolute error) for Yanchi grass, Yanchi crop, 18, 20, 39, and 42 were -1.09, -1.24, -0.85, -0.84, 0.44, and 0.09 °C, respectively. The RMSE (root mean squared error) for Yanchi grass, Yanchi crop, 18, 20, 39, and 42 were 2.68, 2.07, 2.12, 3.28, 2.45, and 2.73 °C, respectively. All single-point simulations at five depths showed high R (>0.95), low BIAS (< ± 1.71 °C), and RMSE (<3.88 °C). As shown in Fig. S3, the R, BIAS, and RMSE between simulated and observed ET in the Yanchi station were 0.93, 15.52, and 17.10 mm month^{-1}, respectively. Fig. S4 shows the spatiotemporal R values between the simulated LST, net radiation, ET, and multiple validation datasets (MODIS and GLASS) for the entire domain. The R for LST, net radiation, and ET were 0.96, 0.84, and 0.83, respectively. Although parameterisation introduced little bias in the performance of the CLM5.0 (Deng et al., 2020; Luo et al., 2020; Ma et al., 2021), LUCC effects suppress model uncertainty due to parameterisation (Tölle et al., 2018). Therefore, CLM5.0 can present a complicated and realistic LUCC in APENWC.

2.5 Criteria of appropriate land use/cover pattern

Considering the importance of warming impacts and the water conservation (WC) function, a proper mixture of land use/cover depends on the LST and WC, which have been introduced as criteria for optimising ecosystem services from the perspective of energy and hydrological cycles (Bai et al., 2019; Zeng and Li, 2019; Wang et al., 2021c). The WC was obtained from the water balance using Eq. (1):

$$WC = P - ET - Runoff \tag{1}$$

where WC is the annual water conservation (mm yr^{-1}). P, ET, and $Runoff$ are the annual precipitation (mm yr^{-1}), evapotranspiration (mm yr^{-1}), and runoff (mm yr^{-1}), respectively. P is the forcing data of CLM5.0, and the other data are the outputs of CLM5.0, whose performance was validated by Li (2021) and in the previous section.

3 Results

3.1 Impacts of LUCC in the APENWC

3.1.1 LUCC from 2000 to 2015

205   To quantify the synergy and respective impacts of different types of LUCC, we first need to examine the local LUCC. From 2000 to 2015, grasslands, evergreen needleleaf forests, deciduous broadleaf forests, and shrublands increased by 7.30, 0.17, 0.15, and 0.07 %, respectively. The bare land and croplands decreased by 8.70 and 0.20 %, respectively. Overall, vegetation coverage in the APENWC increased. The main LUCC consisted of four types: bare land to grasslands 11.62 %, croplands to grasslands 1.18 %, grasslands to bare land 3.83 %, and grasslands to croplands 1.03 %. The conversation off bare land and

210   croplands to grasslands has been driven by vegetation restoration projects in the APENWC. The bare land to grasslands areas were mainly distributed in the northwestern APENWC and were scattered elsewhere, whereas grasslands to bare land occurred in the western APENWC. Croplands to grasslands were principally distributed in the mid-western APENWC and grasslands to croplands were mainly distributed in the mid-southern APENWC.

We focused on the main LUCC: bare land to grasslands, grasslands to bare land, croplands to grasslands, and grasslands to

215   croplands. Meanwhile, grid cells that experienced intense single LUCC type changes ≥ 15 % (Winckler et al., 2018) and other changes ≤ 15 % were selected as representatives for further analysis (Fig. S5).

3.1.2 The impacts of LUCC over the domain

We ran two experiments in CLM5.0 with two land use/covers (2000 and 2015) and static climatic forcing. Fig. 2 shows the spatial and seasonal distributions of temperature differences between CN2015 and EXP2000. The LUCC from 2000 to 2015

220   generally caused a cooling effect in large areas of the APENWC, where the spatially averaged cooling was -0.06 ± 0.15 ℃ (mean ± one standard deviation) due to increased vegetation coverage. Areas towards the eastern part of the APENWC showed a weak effect owing to the slight LUCC in the east (Fig. S5). Seasonally changes were -0.06 ± 0.15 ℃ in spring (MAM: March & April & May), -0.12 ± 0.22 ℃ in summer (JJA: June & July & August), -0.06 ± 0.14 ℃ in autumn (SON: September & October & November) and -0.02 ± 0.17 ℃ in winter (DJF: December & January & February).

225   Similar to the LST, we only considered the changes in ET directly caused by the LUCC with static climatic forcing. The spatial and seasonal distributions of ET differences between CN2015 and EXP2000 are shown in Fig. 3. The LUCC from 2000 to 2015 generally caused an increase in ET in large areas of APENWC, where the difference was 9.70 ± 19.04 mm yr^{-1} as a result of increased vegetation coverage. Seasonally changes were 1.93 ± 4.41 mm season^{-1} in spring, 6.53 ± 11.67 mm season^{-1} in summer, 1.16 ± 3.99 mm season^{-1} in autumn, and 0.07 ± 0.88 mm season^{-1} in winter. The LUCC mainly affected

230   ET in summer, but this trend was weak in autumn and nonexistent in winter.
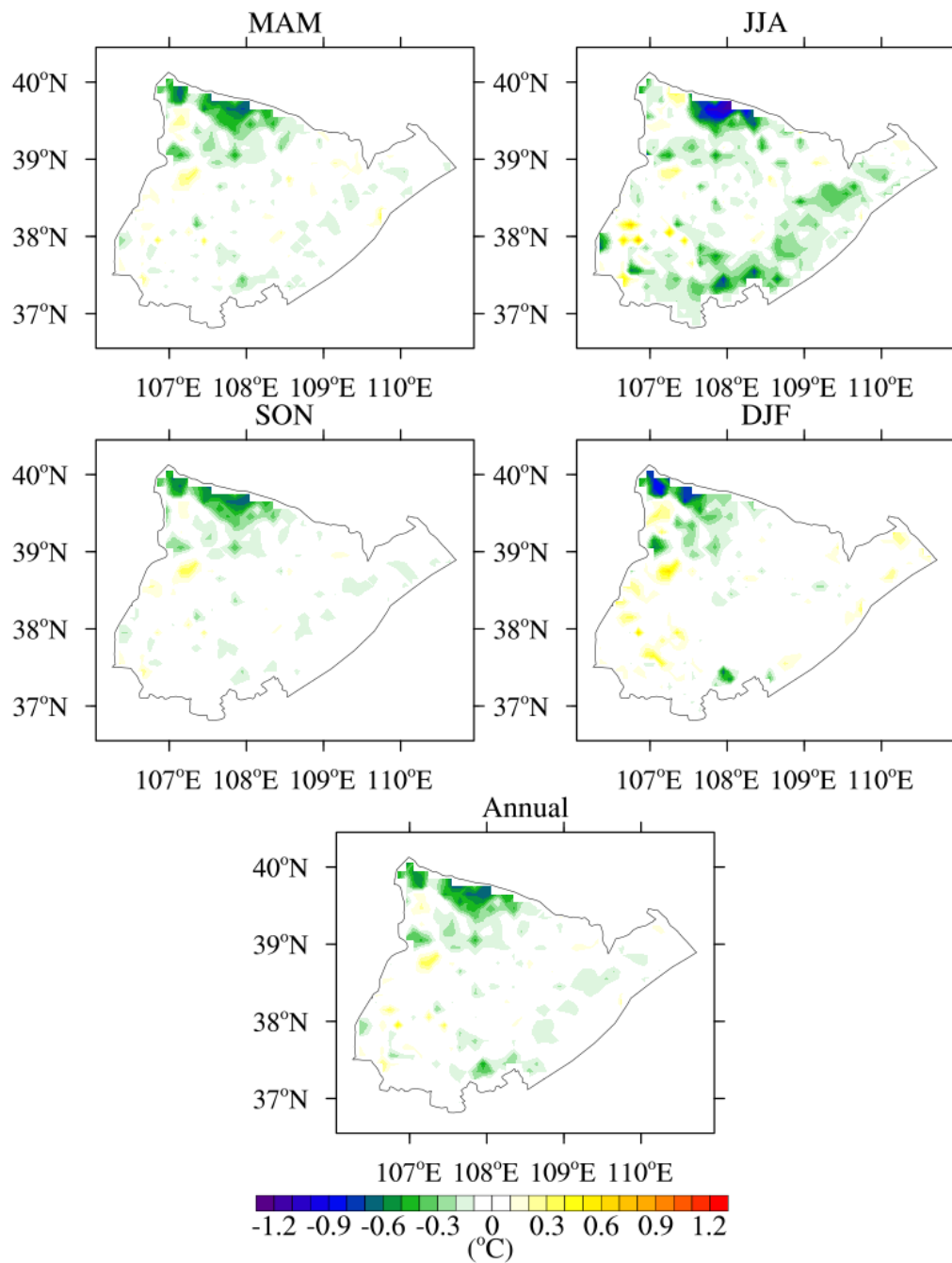
Figure 2. Differences in spatially averaged LST between the simulations with 2000 and 2015 land use data (CN2015 - EXP2000) during MAM, JJA, SON, DJF and annual.

235
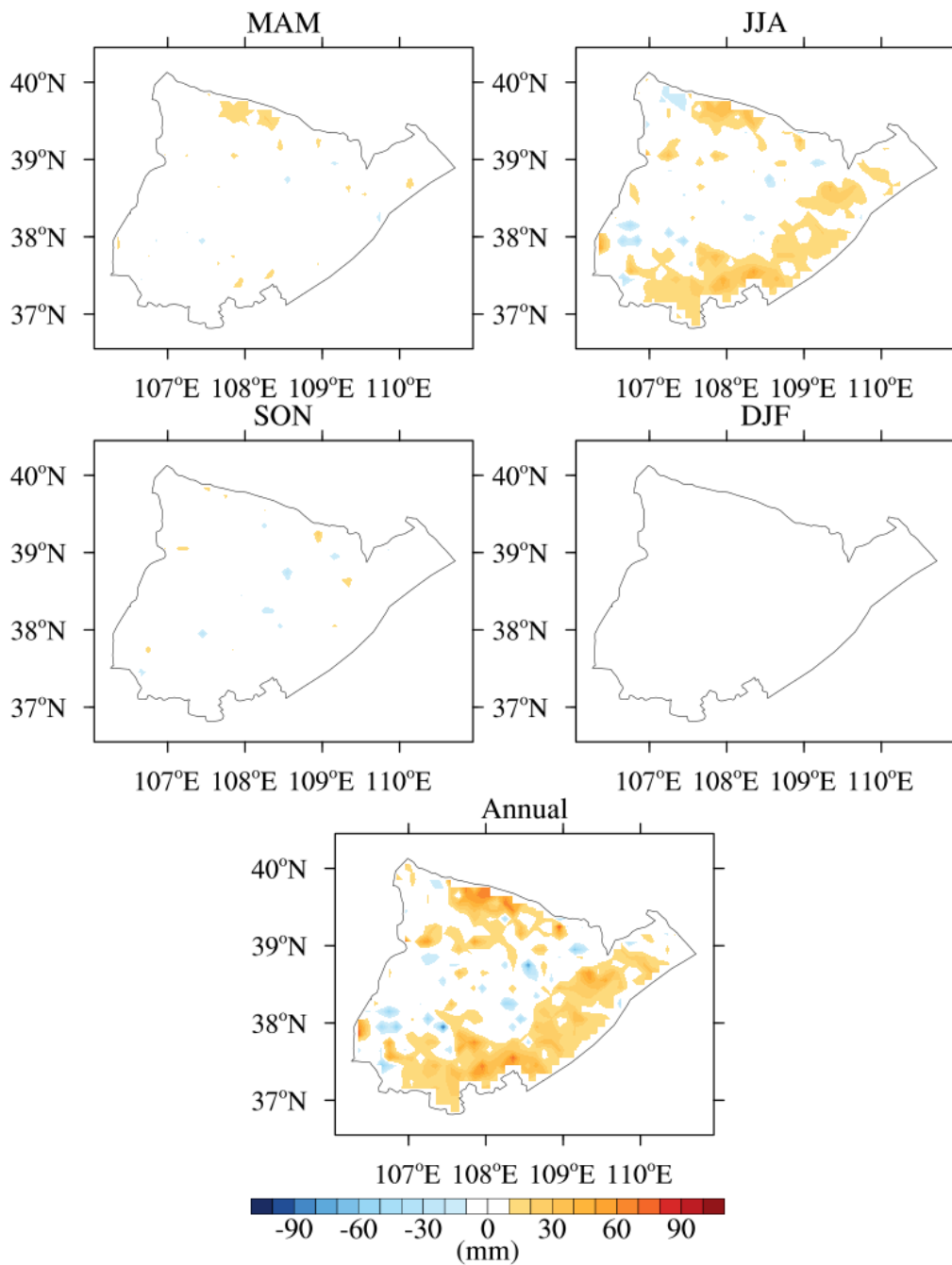
Figure 3. Differences in spatially averaged ET between the simulations with 2000 and 2015 land use data (CN2015 - EXP2000) during MAM, JJA, SON, DJF and annual.

3.1.3 Effects of different LUCC types

Different types of LUCC contribute to different effects and eventually lead to synergistic effects over the domain. To understand the different effects of different types of LUCC, bare land and croplands to grasslands as the two main types of vegetation restoration projects could be carried out through two idealised scenarios. One continent with maximised bare land turned into grasslands, and the other continent with maximized croplands is turned into grasslands (Arora and Montenegro, 2011; Cherubini et al., 2018). Detailed descriptions of these scenarios are presented in Table 1. Analyses of the water and energy processes response to bare land to grasslands were conducted in bare land to grasslands and grasslands to bare land intense grid cells (143 grids; Fig. S5), where bare land and grasslands exist realistically and constantly change back and forth. Similarly, analyses of croplands to grasslands were conducted in croplands to grasslands and grasslands to croplands intense grid cells (10 grids, Fig. S5), where crops and grass can be grown and converted.

The Fig. 4 shows the opposing impacts of the two types of vegetation restoration. The bare land to grasslands reduced the LST by -0.17 °C, an annual average difference. On the contrary, croplands to grasslands led to an increase in LST with an annual average difference of 0.96 °C. From bare land to grasslands scenarios, seasonal average cooling differences were -0.15, -0.74, and -0.66 °C in spring, summer, and autumn, respectively, but warmer in winter with 0.89 °C. Temperature impacts from croplands to grasslands showed a warm effect with a more dramatic variation, with seasonal average differences of 0.08, 2.52, -0.07, and 1.30 °C in spring, summer, autumn, and winter, respectively. Annual changes in ET were 53.32 and -184.42 mm yr^{-1} from bare land and croplands to grasslands, respectively. The differences in ET for bare land to grasslands were 15.67, 23.77, 11.99, and 2.37 mm season^{-1} in spring, summer, fall, and winter, respectively. Conversely, the differences in ET from croplands to grasslands were -34.95, -128.76, -23.48, and 2.76 mm season^{-1} in spring, summer, fall, and winter, respectively. From croplands to grasslands (Table S3) and bare land to grasslands (Table S4), surface albedo was the most sensitive factor. It was significantly correlated with LST and ET in summer and winter. The correlation coefficients in Table S3 further indicate that LAI + SAI was the most sensitive factor influencing the LST and ET from croplands to grasslands throughout the year.
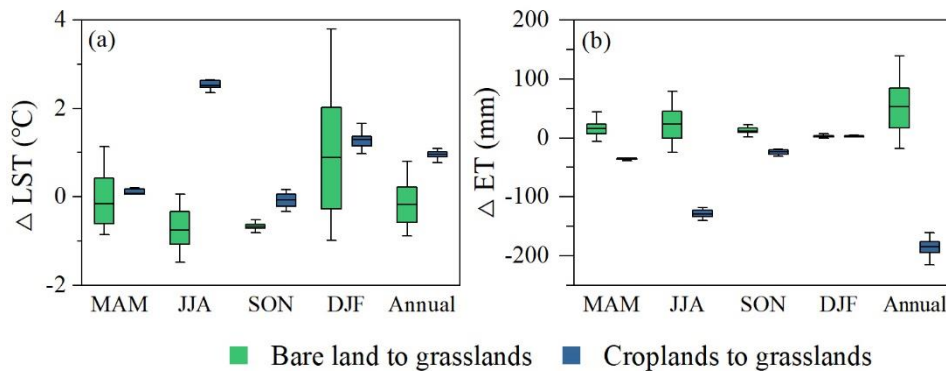
Figure 4. Seasonal changes in LST and ET as box plots from bare land to grasslands (Exp_grass-Exp_bare) and croplands to grasslands (Exp_grass-Exp_crop).

Further analysis focused on the opposing mechanisms of responses of bare land and croplands to grasslands. Complete diurnal cycles were observed only in summer and winter, which are considered the most representative seasons.

a. Bare land to grasslands

In the summer days of CLM5.0 simulations, LST showed cooling from bare land to grasslands (-0.74 ± 0.99 °C, Fig. S6h). The surface temperature was equal to the ground temperature for the bare land. For vegetation cover, the surface temperature is a calculation related to ground and vegetation temperatures (Lawrence et al., 2019). The ground temperature is determined by the amount of energy used to warm the ground and soil, residual heat energy, resulting from the competition between the net radiative energy input and the sum of the turbulent heat fluxes (sensible + latent heat fluxes) (Breil et al., 2020). In Fig. S6f, differences in the ground temperature from bare land to grasslands were relatively small (-0.05 ± 0.48 °C), so the reduced surface temperature from bare land to grasslands was mainly caused by a lower vegetation temperature of grass (Fig. S6g).

In winter, LST increased by 0.89 ± 1.27 °C from bare land to grasslands. The increases in sensible heat fluxes and latent heat fluxes were minimal (Fig. S7b and S7c), indicating increased turbulent term (up to approximately 32 W m^{-2}, Fig. S7d) was compensated by the increased net radiation (up to approximately 52 W m^{-2}, Fig. S7a), suggesting that the net shortwave radiation acted as the primary term. Thus, LST increased as the residual heat increased (up to approximately 21 W m^{-2}, Fig. S7e).

b. Croplands to grasslands

The LST showed warming from croplands to grasslands (2.52 ± 2.35 °C, Fig. S8f). The net radiation decreased from croplands to grasslands (about -40 W m^{-2} at daily maximum, Fig. S8a). The decreased turbulent energy fluxes (about -60 W m^{-2} at daily maximum, Fig. S8d) into the atmosphere were decided by decreased latent heat fluxes (about -133 W m^{-2} at daily maximum, Fig. S8c) rather than increased sensible heat fluxes (approximately 73 W m^{-2} at daily maximum, Fig. S8b).

Ultimately, decreased net radiative energy input was compensated by a decreased sum of turbulent heat fluxes during the day. Thus, the results showed that LST increased during the day as the increased residual heat fluxes (approximately 32 W m^{-2} at the daily maximum, Fig. S8e). At night, the reversed residual ground heat energy hardly reduced the nocturnal LST. This was interpreted as the energy increasing at night not being sufficient to compensate for the higher temperature during the day (Breil et al., 2020).

In winter, the LST increased by 1.30 ± 0.38 °C from croplands to grasslands. No significant differences existed between bare land to grasslands and croplands to grasslands owing to croplands having no vegetation in winter after being managed and being analogous to bare land after harvest in autumn in the CLM.

3.2 Land use/cover pattern in the APENWC

3.2.1 Spatiotemporal mixture of land use/cover

295 To explore the proper mixture of land use/cover, we analysed the mixtures of land use/ cover in 2000 and 2015. The different percentages represent a mixture of land use/cover in each grid. We classified a mixture of land use/cover types. To simplify the classification, only the grids with sum areas of grasslands, bare land, and croplands greater than 90 % were selected. Then the ratio of three main types in each grid represented a mixture of land use/cover.

Fig. 5 shows the spatiotemporal heterogeneity of the land use/cover mixtures for the three main types: grasslands, croplands, 300 and bare land. Each grid had a mixed land use/cover. The different impacts of vegetation restoration from 2000 to 2015 are represented in grids from CN2015 to EXP2000 (Table S5). Different effects of vegetation restoration resulted from the different contributions of the two main types of LUCC: grids from bare land to grasslands led to more cooling and drying; and grids from croplands to grasslands led to more warming and moisture, which is in line with Section 3.1.3. However, a grid from bare land and croplands to grasslands led to more warming and drying owing to the opposing offsetting impacts 305 from croplands to grasslands and bare land to grasslands. Therefore, unclear synergy effects from bare land and croplands to grasslands as vegetation restoration. An appropriate mixture of land use/cover is explored in the next section.
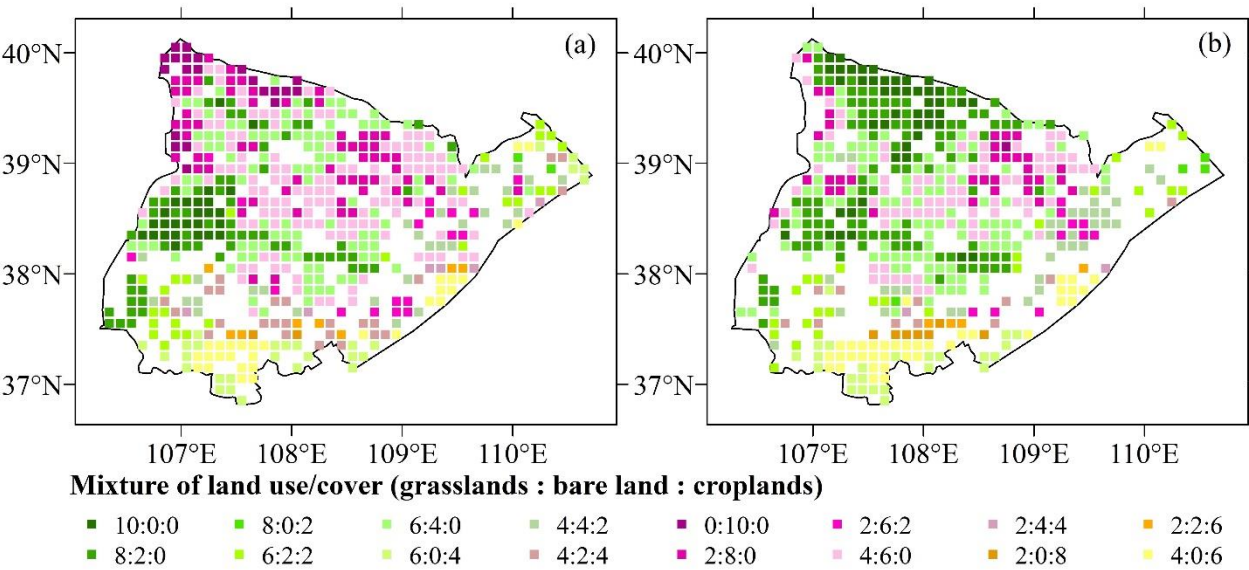
Figure 5. The pattern of land use/cover mixtures in 0.1 ° grids of the study area in 2000 (a), 2015 (b).

3.2.2 Proper mixture of land use/cover for vegetation restoration operations

310 **a. Land use/cover scenarios based on the national ecological plan**

The government plan aims to 1) expand the percentage of grasslands to 60 % and 2) transform bare land and croplands into grasslands(China state council, 2017; National development and reform commission, 2019). Thus, different mixtures of land

use/cover were simulated to pursue the proper mixture of land use/cover. First, we set the percentage of grasslands at 60 %. Then, the percentages of bare land and croplands, 13 and 30 % respectively decreased to meet the increase in grasslands and were set as the maximum in scenarios. Subsequently, five scenarios were selected to reduce computational time. The percentages of grasslands, bare land, and croplands were respectively 60, 21, and 13 % in EXP_602113; 60, 23, and 11 % in EXP_602311; 60, 25, and 9 % in EXP_602509; 60, 27, and 7 % in EXP_602707; 60, 30, and 4 % in EXP_603004 under static climatic forcing.

b. Optimal land use/cover pattern

Comparing the present land use/cover, EXP_602113 and EXP_602311 resulted in a cooling surface, whereas EXP_602509, EXP_602707, and EXP_603004 resulted in a warming surface. Additionally, EXP_602113 induced drying, whereas EXP_602311, EXP_602509, EXP_602707, and EXP_603004 induced high WC (Table 2).

For sustainable ecological construction, it is necessary to pursue an alternative mixture of land use/cover without augmenting warming and endangering water availability. This means the proper mixture of land use/cover has a lower LST and larger WC than in 2015 (Arora and Montenegro, 2011; Bai et al., 2019; Wang et al., 2021d; Findell et al., 2017). Therefore, vegetation restoration strategies in the APENWC should use an appropriate mixture of land use/cover, such as EXP_602311; this indicates that approximately 6.9 % (5348 km^2) of bare land and 1.5 % (1163 km^2) of croplands transformed into grasslands. The LUCC to EXP_602311 generally caused more cooling and slightly increased the WC owing to proper vegetation restoration. Otherwise, other scenarios would lead to warming or drying, exacerbating drought in the APENWC.

Table 2. The spatially weighted averaged differences of LST and WC as different vegetation restoration efforts.

	Δ LST (°C)	Δ WC (mm yr^{-1})
EXP_602113	-0.04	-4.39
EXP_602311	-0.01	0.86
EXP_602509	0.02	6.09
EXP_602707	0.05	11.34
EXP_603004	0.09	19.25

4 Discussion

4.1 Sensitivity of LAI + SAI and vegetation height

In CLM5.0, a dual-source land surface model, the canopy stored energy is zero and is regarded as massless. Vegetation vapour pressure, temperature, and latent heat fluxes are calculated iteratively by the Newton-Raphson method, with high complexity related to several land surface parameters, such as surface albedo, roughness, LAI + SAI, aerodynamic resistance, vegetation height and leaf stomatal resistance (Lawrence et al., 2019). As shown in Fig. 6b, the latent heat fluxes and LST of Yanchi_height and Yanchi_laisai were only slightly different from those of Yanchi_grass and hardly closed to those of Yanchi_crop. Moreover, LAI + SAI and canopy height affected the surface roughness and aerodynamic resistance (Fig. 6g and 6h). This means that complex processes may not simply be adjusted with a single factor and that other characteristics play an indispensable role even though LAI+SAI is the most sensitive factor shown in Table S3. Future work on studying

 of simply considering the correlation between the variables and biogeophysical characteristics.
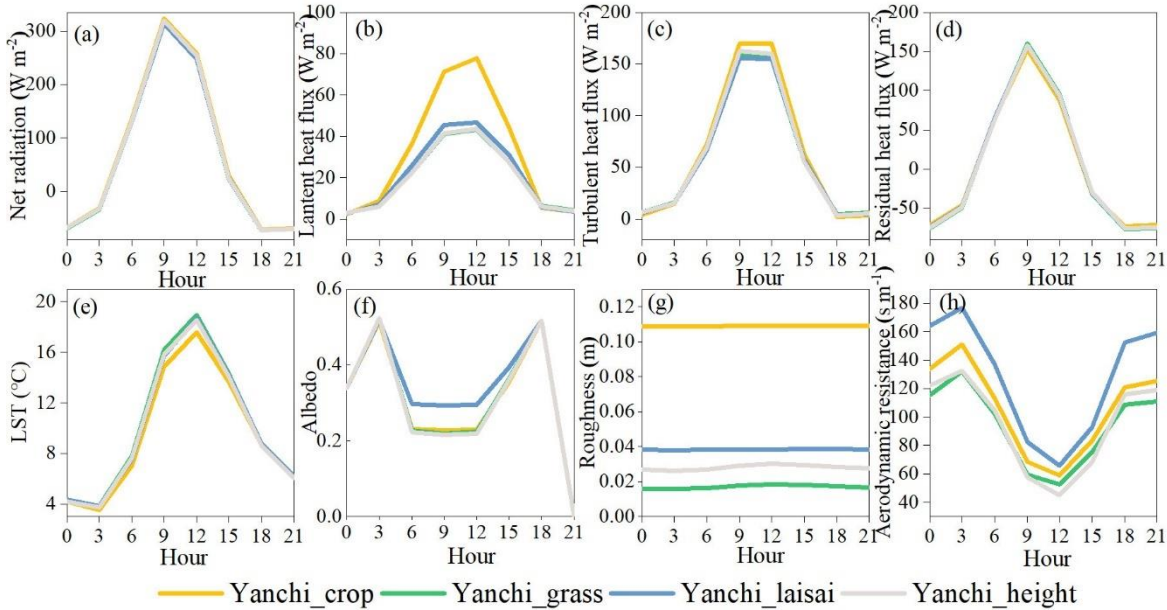
Figure 6. Diurnal cycle (Yanchi_crop & Yanchi_grass & Yanchi_laisai & Yanchi_height, (a) net radiation, (b) latent heat fluxes, (c) turbulent heat fluxes, (d) residual heat fluxes (soil heat fluxes), (e) LST, (f) surface albedo, (g) surface roughness, (h) aerodynamic resistance.

4.2 Uncertainty of soil properties

Land surface processes are mainly presented in the interaction surface of the soil-vegetation-atmosphere (Breil and Schädler, 2017). Soil properties that serve as lower boundary conditions, such as thermal conductivity, porosity and hydraulic conductivity, are key parameters affecting soil moisture, soil temperature and soil heat fluxes which refer to the partitioning of water and energy (Yang et al., 2021b). Although the soil properties dataset for land surface modelling over China provided soil properties with higher precision than the default values of CLM5.0 (Fig. S10), It is worthwhile exploring the uncertainties in modelling the soil input dataset. In Fig. S10, the dataset shows that sand content is less than 60 % and clay content is larger than 10 % in the northwest. However, as experiment data is shown in Table S6, the northwest of the APENWC is a desertified area where the soil contains more mean sand and less mean clay (Duan et al., 2021; Liu et al., 2011; Xu, 2019), implying that discrepancies between the soil dataset and realistic conditions. The conversion of land use/cover leads to changes in soil properties, particularly soil organic matter, sand, and clay content (Celik, 2005; Su et al., 2021). The dynamic changes in soil properties under different land use/cover types were not considered, and the same soil dataset was used before and after the LUCC. Most soil datasets contain soil properties that remain constant for a long time. Thus, the limitation was that the soil properties could not change dynamically with the LUCC, which might have affected the

simulated variables. Therefore, the accuracy of the soil dataset of the study area needs to be improved and a module that considers dynamic changes in soil parameters following the LUCC should be developed in future research.

4.4 Limitations of the study

Ecohydrological sustainability studies the interaction between water and ecological systems, highlighting water as a key driver (Zalewski, 2021). The ecohydrological sustainability related to water consists of water provision, soil erosion, and biodiversity. (1) Water provision. WC is defined as the difference between the income and expenditure of water. It represents the ability of an ecosystem to store or retain water. Therefore, WC represents the amount of water that can be supplied to the region's interior (Bai et al., 2019; Costanza et al., 1997). (2) Soil erosion. Severe soil erosion causes widespread loss of topsoil and the conversion of the once-flat plateau into hills and gullies, leading to catastrophic floods and droughts in the Loess Plateau of China (Chen et al., 2007; Fu et al., 2017). Since the 1980s, vegetation restoration converted sloping (more than 15°) farmland into forests and grasslands, leading to a soil-retention rate of 84.4 % on slopes of 8 °–35 ° (Fu et al., 2017). However, in most APENWC areas, the soil erosion was 0–200 (t km^{-2} yr^{-1}) in 2000 and 2008 (Fu et al., 2011), and the soil erosion rate showed no significant changes during the Grain-for-Green Project (Fu et al., 2017). This is because APNEC is not a gully-hilly area, where intense soil erosion occurs. Therefore, the influence of soil erosion due to vegetation restoration on the ecohydrological sustainability of the APENWC is limited. (3) Biodiversity. During vegetation restoration, the diversity of soil fauna and fungal communities increases, because fast-growing plant species produce large amounts of litter and root exudates, and external resources continually enter the soil food web, promoting nutrient cycling (Wu et al., 2021; Yang et al., 2021c). Water content between 20 and 60 cm soil depths and soil properties can be regarded as the primary factors explaining plant and soil fungal diversity, regardless of land use/cover type (Yang et al., 2017; Wang et al., 2021a). The influence of soil water content on ecohydrological sustainability was included in WC. Additionally, Deng (2022) reported that WC is a crucial factor that needs to be improved in APENWC based on the ecological sustainability evaluation of vegetation restoration. WC has been used as a type of regulating the ecohydrological sustainability due to LUCC (Deng, 2022; Bai et al., 2019; Zeng and Li, 2019). Therefore, the enhancement of ecohydrological sustainability in the study area mainly focuses on improving water conservation.

Previous studies isolated respectively the effects of LUCC and climate change to better understand the water and energy processes in APENWC (Xue et al., 2019; Wang et al., 2020). Yang et al. (2021a) found that vegetation restoration induces soil drying in APENWC. This paper aims to mitigate drying effects by adjusting the mixture of different land use/cover in vegetation restoration. It is the reason why we only consider the impacts of the LUCC. We designed the experiments with different land use cover/use and static climatic forcing. This method has been widely used to eliminate the influence of other factors and isolate the effects of the LUCC (Wang et al., 2021b; Breil et al., 2020). However, the water and energy processes are affected by changes in both LUCC and climate and vegetation-climate coupling is a complex process. It is worthwhile exploring the contribution of background climate in the future study.

Owing to limited in-situ observations, this study validated CLM5.0 with only six stations in the study region. Subsequently, the validated CLM5.0 was used to assess the proposed land use/cover scenarios. Future research needs to verify the proposed

395   scenarios with more diverse in-situ observations before an appropriate land use pattern is selected for implementation at a regional scale.

5 Conclusions

This study first simulated and quantified the effects of LUCC using CLM5.0, which was verified based on in-situ observations, in the agro-pastoral ecotone of northwest China. Subsequently, five LUCC scenarios were proposed and

400   assessed to identify the optimal mixture of land use/cover in the study region. The main findings are as follows: First, bare land to grasslands reduced LST, whereas croplands to grasslands increased LST. Bare land to grasslands caused an increase in ET whereas croplands to grasslands caused a decrease in ET. This led to a spatially averaged cooling surface and increased ET from 2000 to 2015 over the study area. Second, an in-depth analysis of the LUCC pattern from 2000 to 2015 revealed that some grids showed warming or drying, whereas one grid showed both drying and warming. Different mixtures

405   of LUCC could lead to different results for vegetation restoration projects, which indicates the complicated synergistic effects of bare land and croplands to grasslands as vegetation restoration. Finally, assessing the five proposed LUCC scenarios related to the Chinese government's long-term ecological plan based on lowering LST and increasing WC, the optimal mixture of LUCC in the APENWC is approximately 60 % grasslands, 23 % bare land, and 11 % croplands respectively; this suggests that approximately 6.9 % (5348 km^2) of bare land and 1.5 % (1163 km^2) of croplands will be

410   transformed into grasslands to achieve the optimal mixture of LUCC. These findings provide useful information to support land management policy/decision-making in the study region.

Data availability

The data will be made available on request

Authorship contribution

415   Yuzuo Zhu: Conceptualization, Methodology, Software, Validation, Formal analysis, Writing - original draft.
Xuefeng Xu: Data curation, Writing - Review & Editing.

Declaration of competing interest

We declare no competing interest.

Acknowledgments

420 The study was supported by the National Natural Science Foundation of China (grant number: 42030501, 41530752 and 91125010). We thank Prof. Xin Jia and his team at Beijing Forestry University for sharing their in-situ ET observation data from 2015 at Yanchi Station to calibrate the performance of the CLM5.0 in this work.

Reference

Alkama, R. and Cescatti, A.: Biophysical climate impacts of recent changes in global forest cover, Science, 351, 600-604,
425 https://doi.org/10.1126/science.aac8083, 2016.

Arora, V. K. and Montenegro, A.: Small temperature benefits provided by realistic afforestation efforts, Nature Geoscience, 4, 514-518, https://doi.org/10.1038/ngeo1182, 2011.

Bai, Y., Ochuodho, T. O., and Yang, J.: Impact of land use and climate change on water-related ecosystem services in Kentucky, USA, Ecological Indicators, 102, 51-64, https://doi.org/10.1016/j.ecolind.2019.01.079, 2019.

430 Bonan, G. B., Oleson, K. W., Vertenstein, M., Levis, S., Zeng, X., Dai, Y., Dickinson, R. E., and Yang, Z.-L.: The Land Surface Climatology of the Community Land Model Coupled to the NCAR Community Climate Model*, Journal of Climate, 15, 3123-3149, https://doi.org/10.1175/1520-0442(2002)015<3123:Tlscot>2.0.Co;2, 2002.

Breil, M. and Schädler, G.: Quantification of the Uncertainties in Soil and Vegetation Parameterizations for Regional Climate Simulations in Europe, Journal of Hydrometeorology, 18, 1535-1548, https://doi.org/10.1175/jhm-d-16-0226.1,
435 2017.

Breil, M., Rechid, D., Davin, E. L., de Noblet-Ducoudré, N., Katragkou, E., Cardoso, R. M., Hoffmann, P., Jach, L. L., Soares, P. M. M., Sofiadis, G., Strada, S., Strandberg, G., Tölle, M. H., and Warrach-Sagi, K.: The Opposing Effects of Reforestation and Afforestation on the Diurnal Temperature Cycle at the Surface and in the Lowest Atmospheric Model Level in the European Summer, Journal of Climate, 33, 9159-9179, https://doi.org/10.1175/jcli-d-19-0624.1, 2020.

440 Burakowski, E., Tawfik, A., Ouimette, A., Lepine, L., Novick, K., Ollinger, S., Zarzycki, C., and Bonan, G.: The role of surface roughness, albedo, and Bowen ratio on ecosystem energy balance in the Eastern United States, Agricultural and Forest Meteorology, 249, 367-376, https://doi.org/10.1016/j.agrformet.2017.11.030, 2018.

Cai, X., Yang, Z.-L., David, C. H., Niu, G.-Y., and Rodell, M.: Hydrological evaluation of the Noah-MP land surface model for the Mississippi River Basin, Journal of Geophysical Research: Atmospheres, 119, 23-38,
445 https://doi.org/10.1002/2013jd020792, 2014.

Cao, Q., Yu, D., Georgescu, M., Han, Z., and Wu, J.: Impacts of land use and land cover change on regional climate: a case study in the agro-pastoral transitional zone of China, Environmental Research Letters, 10, 124025, https://doi.org/10.1088/1748-9326/10/12/124025, 2015.

Celik, I.: Land-use effects on organic matter and physical properties of soil in a southern Mediterranean highland of Turkey,
450 Soil and Tillage Research, 83, 270-277, https://doi.org/10.1016/j.still.2004.08.001, 2005.

Chen, L. and Dirmeyer, P. A.: Adapting observationally based metrics of biogeophysical feedbacks from land cover/land use change to climate modeling, Environmental Research Letters, 11, 034002, https://doi.org/10.1088/1748-9326/11/3/034002, 2016.

Chen, L. and Dirmeyer, P. A.: Impacts of Land-Use/Land-Cover Change on Afternoon Precipitation over North America,
455 Journal of Climate, 30, 2121-2140, https://doi.org/10.1175/jcli-d-16-0589.1, 2017.

Chen, L. and Dirmeyer, P. A.: Global observed and modelled impacts of irrigation on surface temperature, International Journal of Climatology, 39, 2587-2600, https://doi.org/10.1002/joc.5973, 2018.

Chen, L. and Dirmeyer, P. A.: Differing Responses of the Diurnal Cycle of Land Surface and Air Temperatures to Deforestation, Journal of Climate, 32, 7067-7079, https://doi.org/10.1175/jcli-d-19-0002.1, 2019.

460 Chen, L., Wei, W., Fu, B., and Lü, Y.: Soil and water conservation on the Loess Plateau in China: review and perspective, Progress in Physical Geography: Earth and Environment, 31, 389-403, https://doi.org/10.1177/0309133307081290, 2007.

Cherubini, F., Huang, B., Hu, X., Tölle, M. H., and Strømman, A. H.: Quantifying the climate response to extreme land cover changes in Europe with a regional model, Environmental Research Letters, 13, 074002, https://doi.org/10.1088/1748-9326/aac794, 2018.

465   Notice of the state council on printing and distributing the outline of the national land plan (2016-2035): http://www.gov.cn/zhengce/content/2017-02/04/content_5165309.htm, last access: 2024.

Costanza, R., d'Arge, R., de Groot, R., Farberk, S., Grasso, M., Hannon, B., Limburg, K., Naeem, S., V. O'Neill, R., Paruelo, J., G. Raskin, R., Suttonkk, P., and van den Belt, M.: The value of the world's ecosystem services and natural capital, Nature, 387, 253-259, https://doi.org/10.1038/387253a0, 1997.

470   Das, P., Behera, M. D., Patidar, N., Sahoo, B., Tripathi, P., Behera, P. R., Srivastava, S. K., Roy, P. S., Thakur, P., Agrawal, S. P., and Krishnamurthy, Y. V. N.: Impact of LULC change on the runoff, base flow and evapotranspiration dynamics in eastern Indian river basins during 1985–2005 using variable infiltration capacity approach, Journal of Earth System Science, 127, https://doi.org/10.1007/s12040-018-0921-8, 2018.

Davin, E. L. and de Noblet-Ducoudré, D. N.: Climatic Impact of Global-Scale Deforestation: Radiative versus Nonradiative

475   Processes, Journal of Climate, 23, 97-112, https://doi.org/10.1175/2009jcli3102.1, 2010.

Davin, E. L., Seneviratne, S. I., Ciais, P., Olioso, A., and Wang, T.: Preferential cooling of hot extremes from cropland albedo management, Proc Natl Acad Sci U S A, 111, 9757-9761, https://doi.org/10.1073/pnas.1317323111, 2014.

Davin, E. L., Rechid, D., Breil, M., Cardoso, R. M., Coppola, E., Hoffmann, P., Jach, L. L., Katragkou, E., de Noblet-Ducoudré, N., Radtke, K., Raffa, M., Soares, P. M. M., Sofiadis, G., Strada, S., Strandberg, G., Tölle, M. H., Warrach-Sagi,

480   K., and Wulfmeyer, V.: Biogeophysical impacts of forestation in Europe: first results from the LUCAS (Land Use and Climate Across Scales) regional climate model intercomparison, Earth System Dynamics, 11, 183-200, https://doi.org/10.5194/esd-11-183-2020, 2020.

Deng: Research on ecological performance evaluation of the Sloping Land Conversion Program in the Loess Plateau (in Chinese), Ph.D thesis, Northwest A&F University, 131 pp., 2022.

485   Deng, M., Meng, X., Lyv, Y., Zhao, L., Li, Z., Hu, Z., and Jing, H.: Comparison of Soil Water and Heat Transfer Modeling Over the Tibetan Plateau Using Two Community Land Surface Model (CLM) Versions, Journal of Advances in Modeling Earth Systems, 12, 1942-2466, https://doi.org/10.1029/2020ms002189, 2020.

Ding, X., Zheng, M., and Zheng, X.: The Application of Genetic Algorithm in Land Use Optimization Research: A Review, Land, 10, https://doi.org/10.3390/land10050526, 2021.

490   Du, T., Jiao, J., Duan, H., He, H., XUE, X., and Xie, Y.: Study of conversion between landuse/landcover classification system of Chinese Academy of Science and IGBP classification system: In the northwest argo-pastoral zone Journal of Lanzhou University: Natural Science (in Chinese), 56, 91-95, https://doi.org/10.13885/j.issn.0455-2059.20120.01.011, 2020.

Duan, H., Xie, Y., Du, T., and Wang, X.: Random and systematic change analysis in land use change at the category level-A case study on Mu Us area of China, Sci Total Environ, 777, 145920, https://doi.org/10.1016/j.scitotenv.2021.145920, 2021.

495   Duveiller, G., Hooker, J., and Cescatti, A.: The mark of vegetation change on Earth's surface energy balance, Nat Commun, 9, 679, https://doi.org/10.1038/s41467-017-02810-8, 2018.

Findell, K. L., Berg, A., Gentine, P., Krasting, J. P., Lintner, B. R., Malyshev, S., Santanello, J. A., Jr., and Shevliakova, E.: The impact of anthropogenic land use and land cover change on regional climate extremes, Nat Commun, 8, 989, https://doi.org/10.1038/s41467-017-01038-w, 2017.

500   Fu, B., Liu, Y., Lü, Y., He, C., Zeng, Y., and Wu, B.: Assessing the soil erosion control service of ecosystems change in the Loess Plateau of China, Ecological Complexity, 8, 284-293, https://doi.org/10.1016/j.ecocom.2011.07.003, 2011.

Fu, B., Wang, S., Liu, Y., Liu, J., Liang, W., and Miao, C.: Hydrogeomorphic Ecosystem Responses to Natural and Anthropogenic Changes in the Loess Plateau of China, Annual Review of Earth and Planetary Sciences, 45, 223-243, https://doi.org/10.1146/annurev-earth-063016-020552, 2017.

505   Guo, X., Yao, Y., Zhang, Y., Lin, Y., Jiang, B., Jia, K., Zhang, X., Xie, X., Zhang, L., Shang, K., Yang, J., and Bei, X.: Discrepancies in the Simulated Global Terrestrial Latent Heat Flux from GLASS and MERRA-2 Surface Net Radiation Products, Remote Sensing, 12, 2763, https://doi.org/10.3390/rs12172763, 2020.

Han, Y., Ma, Z., Li, M., and Chen, L.: Numerical simulation of the impact of land use/cover change on land surface process in China from 2001 to 2010, Climatic and Environmental Research (in Chinese), 26, 75-90,

510   https://doi.org/10.3878/j.issn.1006-9585.2020.20039, 2021.

He, Y., Lee, E., and Mankin, J. S.: Seasonal tropospheric cooling in Northeast China associated with cropland expansion, Environmental Research Letters, 15, 034032, https://doi.org/10.1088/1748-9326/ab6616, 2020.

Jia, X., Shao, M., Zhu, Y., and Luo, Y.: Soil moisture decline due to afforestation across the Loess Plateau, China, Journal of Hydrology, 546, 113-122, https://doi.org/10.1016/j.jhydrol.2017.01.011, 2017a.

515 Jia, X., Wang, Y., Shao, M., Luo, Y., and Zhang, C.: Estimating regional losses of soil water due to the conversion of agricultural land to forest in China's Loess Plateau, Ecohydrology, 10, e1851, https://doi.org/10.1002/eco.1851, 2017b.

Kaim, A., Cord, A. F., and Volk, M.: A review of multi-criteria optimization techniques for agricultural land use allocation, Environmental Modelling & Software, 105, 79-93, https://doi.org/10.1016/j.envsoft.2018.03.031, 2018.

Kucsicsa, G., Popovici, E.-A., Bălteanu, D., Grigorescu, I., Dumitraşcu, M., and Mitrică, B.: Future land use/cover changes

520 in Romania: regional simulations based on CLUE-S model and CORINE land cover database, Landscape and Ecological Engineering, 15, 75-90, https://doi.org/10.1007/s11355-018-0362-1, 2019.

Kueppers, L. M. and Snyder, M. A.: Influence of irrigated agriculture on diurnal surface energy and water fluxes, surface climate, and atmospheric circulation in California, Climate Dynamics, 38, 1017-1029, https://doi.org/10.1007/s00382-011-1123-0, 2011.

525 Lawrence, D. M., Fisher, R. A., Koven, C. D., Oleson, K. W., Swenson, S. C., Bonan, G., Collier, N., Ghimire, B., Kampenhout, L., Kennedy, D., Kluzek, E., Lawrence, P. J., Li, F., Li, H., Lombardozzi, D., Riley, W. J., Sacks, W. J., Shi, M., Vertenstein, M., Wieder, W. R., Xu, C., Ali, A. A., Badger, A. M., Bisht, G., Broeke, M., Brunke, M. A., Burns, S. P., Buzan, J., Clark, M., Craig, A., Dahlin, K., Drewniak, B., Fisher, J. B., Flanner, M., Fox, A. M., Gentine, P., Hoffman, F., Keppel-Aleks, G., Knox, R., Kumar, S., Lenaerts, J., Leung, L. R., Lipscomb, W. H., Lu, Y., Pandey, A., Pelletier, J. D.,

530 Perket, J., Randerson, J. T., Ricciuto, D. M., Sanderson, B. M., Slater, A., Subin, Z. M., Tang, J., Thomas, R. Q., Val Martin, M., and Zeng, X.: The Community Land Model Version 5: Description of New Features, Benchmarking, and Impact of Forcing Uncertainty, Journal of Advances in Modeling Earth Systems, 11, 4245-4287, https://doi.org/10.1029/2018ms001583, 2019.

Lee, X., Goulden, M. L., Hollinger, D. Y., Barr, A., Black, T. A., Bohrer, G., Bracho, R., Drake, B., Goldstein, A., Gu, L.,

535 Katul, G., Kolb, T., Law, B. E., Margolis, H., Meyers, T., Monson, R., Munger, W., Oren, R., Paw, U. K., Richardson, A. D., Schmid, H. P., Staebler, R., Wofsy, S., and Zhao, L.: Observed increase in local cooling effect of deforestation at higher latitudes, Nature, 479, 384-387, https://doi.org/10.1038/nature10588, 2011.

Li, F.: Assessment and fusion of the soil moisture data sets based on community land model and smap satellite (in Chinese), M.S. thesis, Lanzhou Univeristy, 16-40 pp., 2021.

540 Li, G., Zhang, F., Jing, Y., Liu, Y., and Sun, G.: Response of evapotranspiration to changes in land use and land cover and climate in China during 2001-2013, Sci Total Environ, 596-597, 256-265, https://doi.org/10.1016/j.scitotenv.2017.04.080, 2017.

Li, X., Yang, L., Tian, W., Xu, X., and He, C.: Land use and land cover change in agro-pastoral ecotone in Northern China: A review, Chinese Journal of Applied Ecology (in Chinese), 29, 3487-3495, https://doi.org/10.13287/j.1001-

545 9332.201810.020, 2018.

Li, X., Xu, X., Wang, X., Xu, S., Tian, W., Tian, J., and He, C.: Assessing the Effects of Spatial Scales on Regional Evapotranspiration Estimation by the SEBAL Model and Multiple Satellite Datasets: A Case Study in the Agro-Pastoral Ecotone, Northwestern China, Remote Sensing, 13, 1524, https://doi.org/10.3390/rs13081524, 2021.

Li, Y., Zhao, M., Motesharrei, S., Mu, Q., Kalnay, E., and Li, S.: Local cooling and warming effects of forests based on

550 satellite observations, Nat Commun, 6, 6603, https://doi.org/10.1038/ncomms7603, 2015.

Liang, W., Bai, D., Wang, F., Fu, B., Yan, J., Wang, S., Yang, Y., Long, D., and Feng, M.: Quantifying the impacts of climate change and ecological restoration on streamflow changes based on a Budyko hydrological model in China's Loess Plateau, Water Resources Research, 51, 6500-6519, https://doi.org/10.1002/2014wr016589, 2015.

Liu, J., Shao, Q., Yan, X., Fan, J., Zhan, J., Deng, X., Kuang, W., and Huang, L.: The climatic impacts of land use and land

555 cover change compared among countries, Journal of Geographical Sciences, 26, 889-903, https://doi.org/10.1007/s11442-016-1305-0, 2016.

Liu, P., Zha, T., Jia, X., Black, T. A., Jassal, R. S., Ma, J., Bai, Y., and Wu, Y.: Different Effects of Spring and Summer Droughts on Ecosystem Carbon and Water Exchanges in a Semiarid Shrubland Ecosystem in Northwest China, Ecosystems, 22, 1869-1885, https://doi.org/10.1007/s10021-019-00379-5, 2019.

560   Liu, Y., Li, J., and Bao, Y.: Dynamic analysis of desertification in the western of Ordos Plateau-The case of Etoke Banner, Journal of Inner Mongolia Agricultural University (In Chinese), 32, 81-87, https://doi.org/CNKI:SUN:NMGM.0.2011-04-017, 2011.

Llopart, M., Reboita, M., Coppola, E., Giorgi, F., da Rocha, R., and de Souza, D.: Land Use Change over the Amazon Forest and Its Impact on the Local Climate, Water, 10, 149, https://doi.org/10.3390/w10020149, 2018.

565   Luo, Q., Wen, J., Hu, Z., Lu, Y., and Yang, X.: Parameter Sensitivities of the Community Land Model at Two Alpine Sites in the Three-River Source Region, Journal of Meteorological Research, 34, 851-864, https://doi.org/10.1007/s13351-020-9205-8, 2020.

Ma, X., Jin, J., Zhu, L., and Liu, J.: Evaluating and improving simulations of diurnal variation in land surface temperature with the Community Land Model for the Tibetan Plateau, PeerJ, 9, e11040, https://doi.org/10.7717/peerj.11040, 2021.

570   Meier, R., Davin, E. L., Lejeune, Q., Hauser, M., Li, Y., Martens, B., Schultz, N. M., Sterling, S., and Thiery, W.: Evaluating and improving the Community Land Model's sensitivity to land cover, Biogeosciences, 15, 4731-4757, https://doi.org/10.5194/bg-15-4731-2018, 2018.

Major projects for ecological protection and restoration support systems: http://gi.mnr.gov.cn/202006/t20200611_2525741.html, last access: 2024.

575   Ning, J., Gao, Z., and Xu, F.: Effects of land cover change on evapotranspiration in the Yellow River Delta analyzed with the SEBAL model, Journal of Applied Remote Sensing, 11, 016009, https://doi.org/10.1117/1.Jrs.11.016009, 2017.

Nkhoma, L., Ngongondo, C., Dulanya, Z., and Monjerezi, M.: Evaluation of integrated impacts of climate and land use change on the river flow regime in Wamkurumadzi River, Shire Basin in Malawi, Journal of Water and Climate Change, 12, 1674-1693, https://doi.org/10.2166/wcc.2020.138, 2021.

580   Poniatowski, D., Beckmann, C., Löffler, F., Münsch, T., Helbing, F., Samways, M. J., Fartmann, T., and Lancaster, L.: Relative impacts of land-use and climate change on grasshopper range shifts have changed over time, Global Ecology and Biogeography, 29, 2190-2202, https://doi.org/10.1111/geb.13188, 2020.

Shangguan, W. and Dai, Y.: A China Dataset of soil hydraulic parameters pedotransfer functions for land surface modeling (1980), National Tibetan Plateau/Third Pole Environment Data Center [data set], https://doi.org/10.11888/Soil.tpdc.270281,

585   2013.

Srivastava, P. K., Han, D., Islam, T., Petropoulos, G. P., Gupta, M., and Dai, Q.: Seasonal evaluation of evapotranspiration fluxes from MODIS satellite and mesoscale model downscaled global reanalysis datasets, Theoretical and Applied Climatology, 124, 461-473, https://doi.org/10.1007/s00704-015-1430-1, 2015.

Su, Y., Zhang, Y., Shang, L., Wang, S., Hu, G., Song, M., and Zhou, K.: Root-induced alterations in soil hydrothermal

590   properties in alpine meadows of the Qinghai-Tibet Plateau, Rhizosphere, 20, 2176, https://doi.org/10.1016/j.rhisph.2021.100451, 2021.

Tan, X., Zhang, L., He, C., Zhu, Y., Han, Z., and Li, X.: Applicability of cosmic-ray neutron sensor for measuring soil moisture at the agricultural-pastoral ecotone in northwest China, Science China Earth Sciences, 63, 1730-1744, https://doi.org/10.1007/s11430-020-9650-2, 2020.

595   Tölle, M. H., Breil, M., Radtke, K., and Panitz, H.-J.: Sensitivity of European Temperature to Albedo Parameterization in the Regional Climate Model COSMO-CLM Linked to Extreme Land Use Changes, Frontiers in Environmental Science, 6, 123, https://doi.org/10.3389/fenvs.2018.00123, 2018.

Wan, Z., Hook, S., and Hulley, G.: MOD11C1 (6), NASA [data set], https://doi.org/10.5067/MODIS/MOD11C1.006, 2015.

Wang, H., Xiao, W., Zhao, Y., Wang, Y., Hou, B., Zhou, Y., Yang, H., Zhang, X., and Cui, H.: The Spatiotemporal

600   Variability of Evapotranspiration and Its Response to Climate Change and Land Use/Land Cover Change in the Three Gorges Reservoir, Water, 11, 1739, https://doi.org/10.3390/w11091739, 2019a.

Wang, L., Wang, X., Chen, L., Song, N. P., and Yang, X. G.: Trade-off between soil moisture and species diversity in semi-arid steppes in the Loess Plateau of China, Sci Total Environ, 750, 141646, https://doi.org/10.1016/j.scitotenv.2020.141646, 2021a.

605   Wang, W., Sun, L., and Luo, Y.: Changes in Vegetation Greenness in the Upper and Middle Reaches of the Yellow River Basin over 2000–2015, Sustainability, 11, 2176, https://doi.org/10.3390/su11072176, 2019b.

Wang, X., Zhang, B., Xu, X., Tian, J., and He, C.: Regional water-energy cycle response to land use/cover change in the agro-pastoral ecotone, Northwest China, Journal of Hydrology, 580, 124246, https://doi.org/10.1016/j.jhydrol.2019.124246, 2020.

610   Wang, X., Zhang, B., Li, F., Li, X., Li, X., Wang, Y., Shao, R., Tian, J., and He, C.: Vegetation restoration projects intensify intraregional water recycling processes in the agro-pastoral ecotone of Northern China, Journal of Hydrometeorology, https://doi.org/10.1175/jhm-d-20-0125.1, 2021b.

Wang, Y., Ye, Z., Qiao, F., Li, Z., Miu, C., Di, Z., and Gong, W.: Review on connotation and estimation method of water conservation, South-to-North Water Transfers and Water Science & Technology (in Chinese), 19, 1041-2017,
615   https://doi.org/10.23476/j.cnki.nsbdqk.2021.0109, 2021c.

Wang, Z., Cao, J., and Yang, H.: Multi-Time Scale Evaluation of Forest Water Conservation Function in the Semiarid Mountains Area, Forests, 12, 116, https://doi.org/10.3390/f12020116, 2021d.

Wei, B., Xie, Y., Jia, X., Wang, X., He, H., and Xue, X.: Land use/land cover change and it's impacts on diurnal temperature range over the agricultural pastoral ecotone of Northern China, Land Degradation & Development, 29, 3009-3020,
620   https://doi.org/10.1002/ldr.3052, 2018.

Winckler, J., Reick, C. H., and Pongratz, J.: Robust Identification of Local Biogeophysical Effects of Land-Cover Change in a Global Climate Model, Journal of Climate, 30, 1159-1176, https://doi.org/10.1175/jcli-d-16-0067.1, 2017.

Winckler, J., Reick, C. H., Luyssaert, S., Cescatti, A., Stoy, P. C., Lejeune, Q., Raddatz, T., Chlond, A., Heidkamp, M., and Pongratz, J.: Different response of surface temperature and air temperature to deforestation in climate models, Earth System
625   Dynamics Discussions, 1-17, https://doi.org/10.5194/esd-2018-66, 2018.

Woodward, C., Shulmeister, J., Larsen, J., Jacobsen, G. E., and Zawadzki, A.: The hydrological legacy of deforestation on global wetlands, Science 346, 844-847, https://doi.org/10.1126/science.1260510, 2014.

Wu, Y., Chen, W., Entemake, W., Wang, J., Liu, H., Zhao, Z., Li, Y., Qiao, L., Yang, B., Liu, G., and Xue, S.: Long-term vegetation restoration promotes the stability of the soil micro-food web in the Loess Plateau in North-west China, Catena,
630   202, https://doi.org/10.1016/j.catena.2021.105293, 2021.

Wu, Z., Wu, J., Liu, J., He, B., Lei, T., and Wang, Q.: Increasing terrestrial vegetation activity of ecological restoration program in the Beijing–Tianjin Sand Source Region of China, Ecological Engineering, 52, 37-50, https://doi.org/10.1016/j.ecoleng.2012.12.040, 2013.

Xu, X.: Ningxia statistical yearbook, China Statistic Press, 381 pp., ISBN 978-7-5037-8514-6, 2018.
635   Xu, X., Li, X., Wang, X., He, C., Tian, W., Tian, J., and Yang, L.: Estimating daily evapotranspiration in the agricultural-pastoral ecotone in Northwest China: A comparative analysis of the Complementary Relationship, WRF-CLM4.0, and WRF-Noah methods, Sci Total Environ, 729, 138635, https://doi.org/10.1016/j.scitotenv.2020.138635, 2020.

Xu, Z.: Study on ecological environment influencing factors and comprehensive evaluation of typical pastoral areas in western China (in Chinese), M.S. thesis, Xi'an University of Technology, 38-39 pp., 2019.
640   Xue, Y., Zhang, B., He, C., and Shao, R.: Detecting Vegetation Variations and Main Drivers over the Agropastoral Ecotone of Northern China through the Ensemble Empirical Mode Decomposition Method, Remote Sensing, 11, 1860, https://doi.org/10.3390/rs11161860, 2019.

Yang, J.: Ordos statistical yearbook, China Statistics Press, 180 pp., ISBN 978-7-5037-8711-9, 2021.

Yang, K. and He, J.: China meteorological forcing dataset (1979-2018), National Tibetan Plateau/Third Pole Environment
645   Data Center [data set], https://doi.org/10.11888/AtmosphericPhysics.tpe.249369.file, 2016.

Yang, L., Horion, S., He, C., and Fensholt, R.: Tracking Sustainable Restoration in Agro-Pastoral Ecotone of Northwest China, Remote Sensing, 13, 5031, https://doi.org/10.3390/rs13245031, 2021a.

Yang, L., Xie, Y., Zong, L., Qiu, T., and Jiao, J.: Land use optimization configuration based on multi- objective genetic algorithm and FLUS model of agro- pastoral ecotone in Northwest China, Journal of Geo-information Science (in Chinese),
650   22, 568-579, https://doi.org/10.12082/dqxxkx.2020.190531, 2020.

Yang, S., Li, R., Wu, T., Wu, X., Zhao, L., Hu, G., Zhu, X., Du, Y., Xiao, Y., Zhang, Y., Ma, J., Du, E., Shi, J., and Qiao, Y.: Evaluation of soil thermal conductivity schemes incorporated into CLM5.0 in permafrost regions on the Tibetan Plateau, Geoderma, 401, 115330, https://doi.org/10.1016/j.geoderma.2021.115330, 2021b.

Yang, X., Shao, M. a., Li, T., Gan, M., and Chen, M.: Community characteristics and distribution patterns of soil fauna after
655   vegetation restoration in the northern Loess Plateau, Ecological Indicators, 122, https://doi.org/10.1016/j.ecolind.2020.107236, 2021c.

Yang, Y., Dou, Y., Huang, Y., and An, S.: Links between Soil Fungal Diversity and Plant and Soil Properties on the Loess Plateau, Frontiers in Microbiology, 8, https://doi.org/10.3389/fmicb.2017.02198, 2017.

Yang, Z. L., Dickinson, R. E., Henderson-Sellers, A., and Pitman, A. J.: Preliminary study of spin-up processes in land surface models with the first stage data of Project for Intercomparison of Land Surface Parameterization Schemes Phase 1(a), Journal of Geophysical Research, 100, 16553-16578, https://doi.org/10.1029/95jd01076, 1995.

Yao, Y., Liang, S., Li, X., Hong, Y., Fisher, J. B., Zhang, N., Chen, J., Cheng, J., Zhao, S., Zhang, X., Jiang, B., Sun, L., Jia, K., Wang, K., Chen, Y., Mu, Q., and Feng, F.: Bayesian multimodel estimation of global terrestrial latent heat flux from eddy covariance, meteorological, and satellite observations, Journal of Geophysical Research: Atmospheres, 119, 4521-4545, https://doi.org/10.1002/2013jd020864, 2014.

Zalewski, M.: Ecohydrology: An Integrative Sustainability Science, London, UK: IntechOpen, 53-61 pp., 2021.

Zeng, L. and Li, J.: A Bayesian belief network approach for mapping water conservation ecosystem service optimization region, Journal of Geographical Sciences, 29, 1021-1038, https://doi.org/10.1007/s11442-019-1642-x, 2019.

Zhang, K., Kimball, J. S., Nemani, R. R., and Running, S. W.: A continuous satellite-derived global record of land surface evapotranspiration from 1983 to 2006, Water Resources Research, 46, W09522, https://doi.org/10.1029/2009wr008800, 2010.

Zhang, L., He, C., Tian, W., and Zhu, Y.: Evaluation of Precipitation Datasets from TRMM Satellite and Down-scaled Reanalysis Products with Bias-correction in Middle Qilian Mountain, China, Chinese Geographical Science, 31, 474-490, https://doi.org/10.1007/s11769-021-1205-9, 2021.

Zhang, S., Yang, H., Yang, D., and Jayawardena, A. W.: Quantifying the effect of vegetation change on the regional water balance within the Budyko framework, Geophysical Research Letters, 43, 1140-1148, https://doi.org/10.1002/2015gl066952, 2016.

Zhang, S., Yang, D., Yang, Y., Piao, S., Yang, H., Lei, H., and Fu, B.: Excessive Afforestation and Soil Drying on China's Loess Plateau, Journal of Geophysical Research: Biogeosciences, 123, 923-935, https://doi.org/10.1002/2017jg004038, 2018.